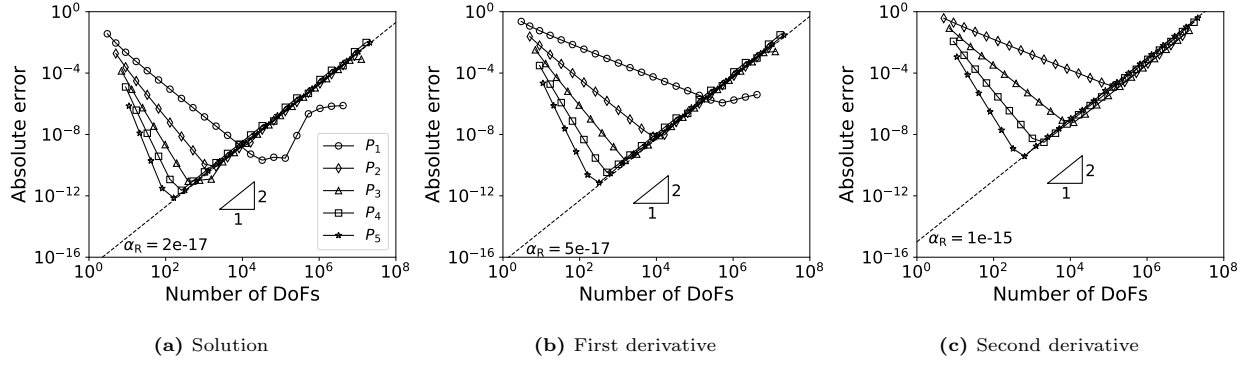


## 1. Numerical results for the benchmark Poisson, diffusion and Helmholtz equations

### 1.1. The Poisson equation

#### 1.1.1. $p$ variant



**Fig. 1.** Absolute errors for the benchmark Poisson equation using the standard FEM.

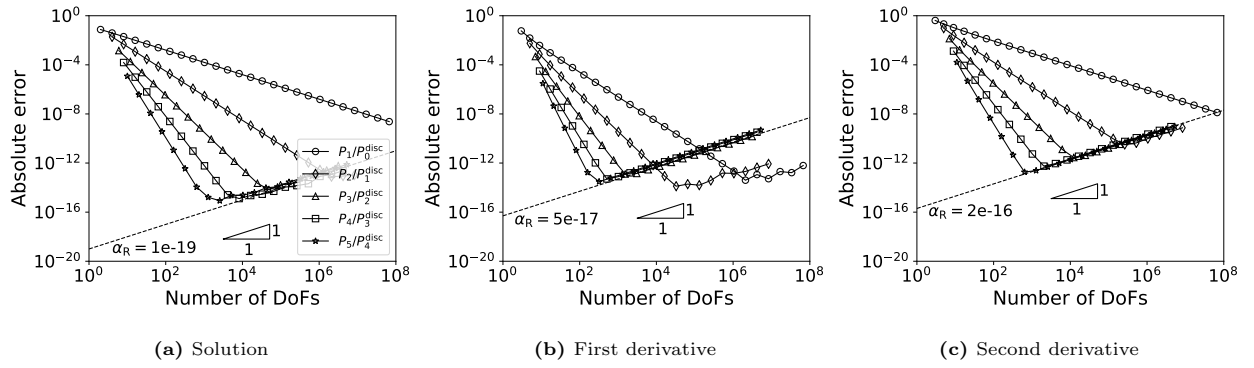


**Fig. 2.** Absolute errors for the benchmark Poisson equation using the mixed FEM.

### 1.2. The diffusion equation for $p = (2\pi c_1)^{-2} \sin(2\pi c_1 x)$ , $d = 10$

The standard FEM.

The mixed FEM.

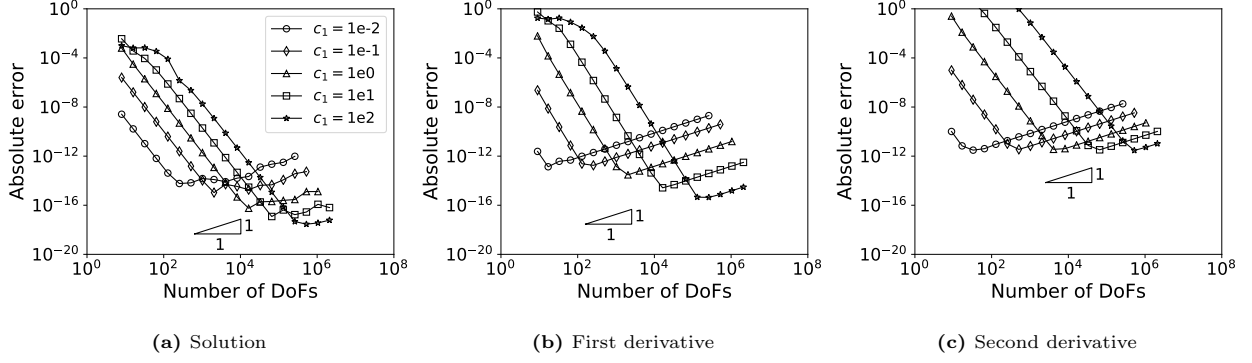


**Fig. 3.** Absolute errors for the diffusion equation with  $p = (2\pi c_1)^{-2} \sin(2\pi c_1 x)$ ,  $d = 10$  using the mixed FEM, no scaling.

### 1.3. The diffusion equation for $p = \sin(2\pi x)$ , $d = 1 + 0.5 \sin(cx)$

To investigate the influence of the oscillation of the diffusion coefficient on the error, we consider  $d = 1 + \frac{1}{2} \sin(cx)$  for the benchmark Poisson equation, resulting the first diffusion equation. For  $c$  ranging from 1 to  $10^4$ ,  $\|d\|_2$  is of order 1, see Fig. 4. The oscillation of  $d$  magnifies when  $c$  increases. Using both the standard FEM and the mixed FEM, the errors are shown below. For the standard FEM,  $P_2$  elements are used, and for the mixed FEM,  $P_4/P_3^{\text{disc}}$  elements are used.

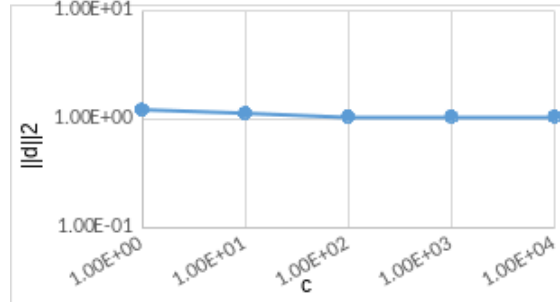


**Fig. 4.** Change of  $\|d\|_2$  with the coefficient  $c$  for the first diffusion equation.

*The standard FEM.* The truncation error increases when the  $d$  oscillates relatively large, i.e. when  $c$  is larger than 10. The lines approximating the round-off error for the solution and first derivative are not affected by the oscillation of  $d$ , but that for the second derivative moves up a bit when  $c$  is larger than 10.

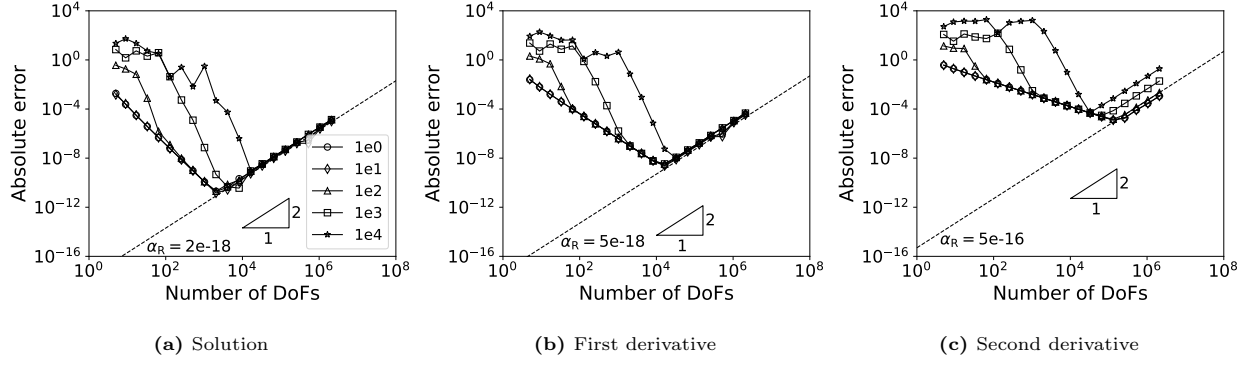


**Fig. 5.** Absolute errors for the first diffusion equation using the standard FEM.

*The mixed FEM.* The truncation error increases when  $d$  oscillates relatively large. The lines approximating the round-off error are not affected.

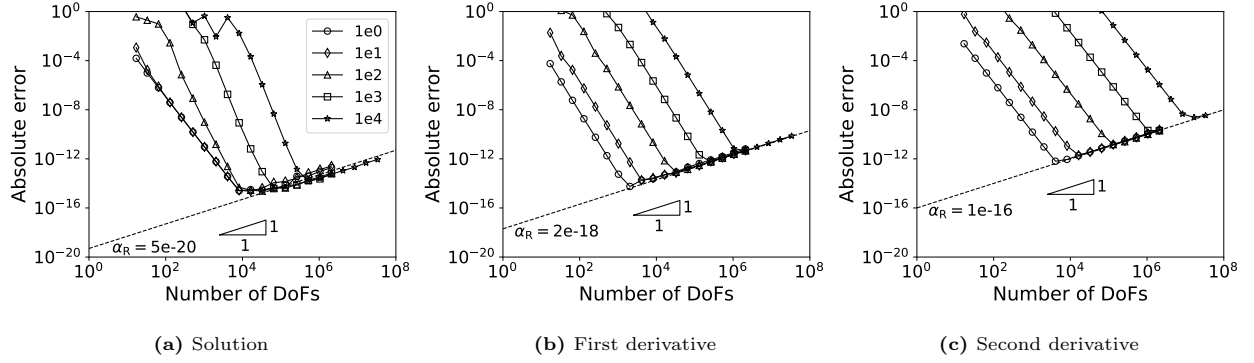


**Fig. 6.** Absolute errors for the first diffusion equation using the mixed FEM.

Last but not least, the offsets  $\alpha_R$  tend to be smaller than that of the Poisson equation.

#### 1.4. The diffusion equation for $p=\sin(2\pi x)$ , $d=1+cx$

We consider the diffusion equation shown in Table 1 in [1]. We first find the offsets  $\alpha_R$  for the diffusion equation using recommended scaling schemes for the standard and mixed FEMs, in which the element degree  $p$  ranges from 1 to 5. Next, we investigate  $\alpha_R$  for different coefficients, i.e.  $d(x) = 1 + cx$  with  $c$  ranging from  $10^{-4}$  to  $10^4$ , in which  $P_2$  elements are used for the standard FEM, and  $P_4/P_3^{\text{disc}}$  elements are used for the mixed FEM.

##### 1.4.1. $p$ variant

*The standard FEM.* Not using scaling and using scheme  $S$ , the errors are shown in Fig. 7.

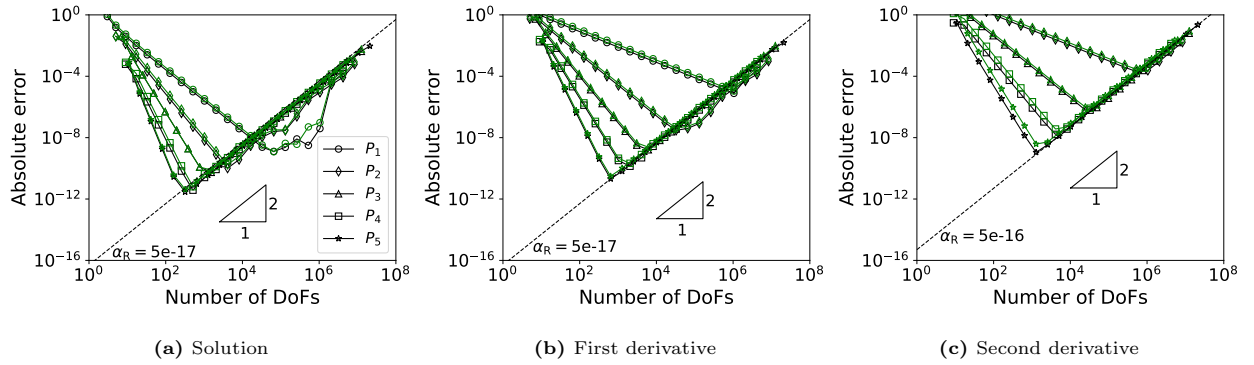


**Fig. 7.** Absolute errors for the benchmark diffusion equation using the standard FEM. The black color denotes results without scaling, and the green color denotes results using scheme  $S$ .

*The mixed FEM.* Not using scaling and using schemes  $M_1$  and  $M_2$ , the errors are shown in Fig. 8.

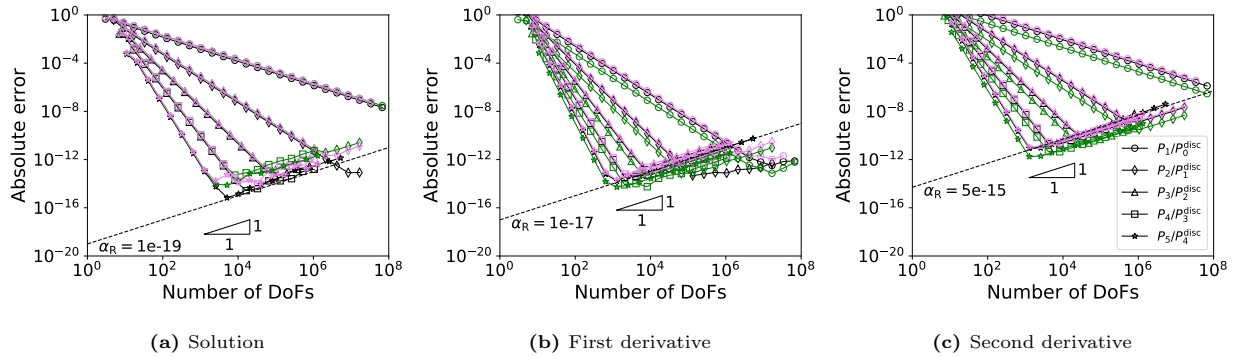


**Fig. 8.** Absolute errors for the benchmark diffusion equation using the mixed FEM. The black color denotes results without scaling, the green color denotes results using scheme  $M_1$  and the violet color denotes results using scheme  $M_2$ .

The offsets  $\alpha_R$  for different scaling schemes are summarized in Fig. 9. For the standard FEM,  $\alpha_R$  are basically the same using scheme  $S$  or not. For the mixed FEM,  $\alpha_R$  changes a bit for different scaling schemes.

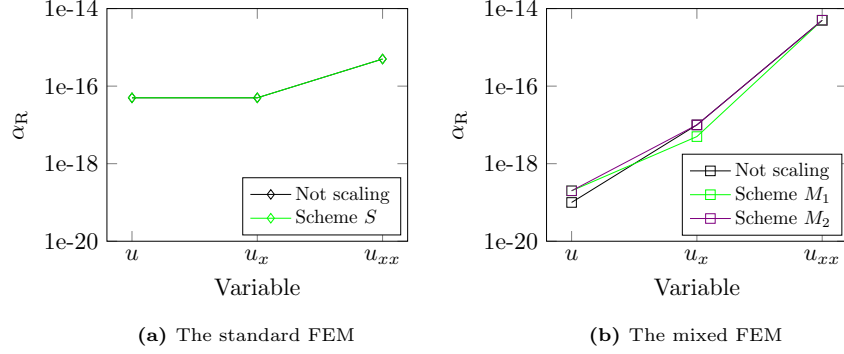


**Fig. 9.**  $\alpha_R$  for the benchmark diffusion equation for different scaling schemes.

#### 1.4.2. $c$ variant

The values of  $\|d\|_2$  for different  $c$  are given in Fig. 10. It shows that when  $c < 1$ ,  $\|d\|_2$  are basically the same; when  $c > 1$ ,  $\|d\|_2$  increases quickly.

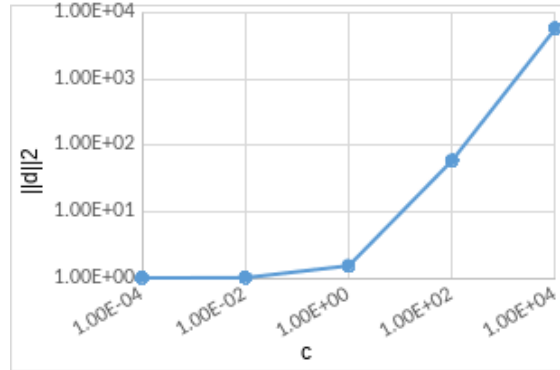


**Fig. 10.** Change of  $\|d\|_2$  with the coefficient  $c$  for the diffusion equation.

*The standard FEM.* Using scheme  $S$ , the errors are shown in Fig. 11. When  $c < 1$ , like  $\|d\|_2$ ,  $\alpha_R$  for different  $c$  are basically the same; when  $c > 1$ ,  $\alpha_R$  increases with  $c$ , and the magnitude of the increase is larger for higher-order derivatives.

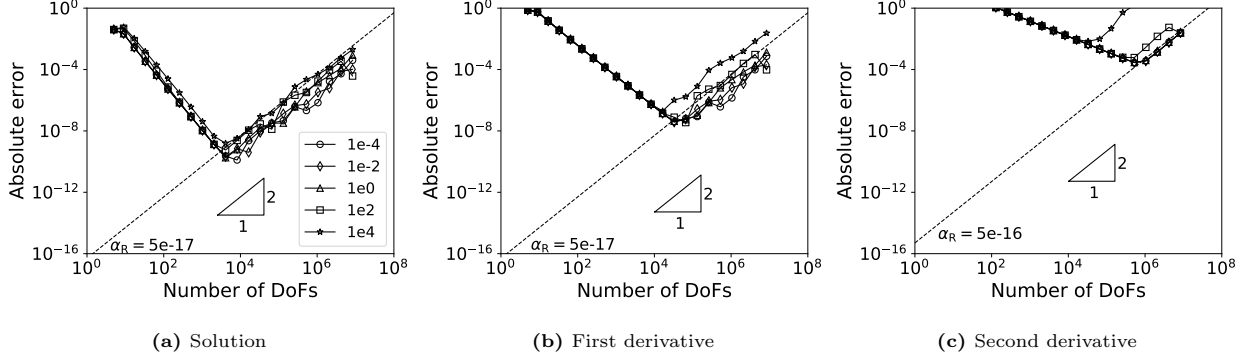


**Fig. 11.** Absolute errors for the benchmark diffusion equation using the standard FEM with scheme  $S$ ,  $c$  variant.

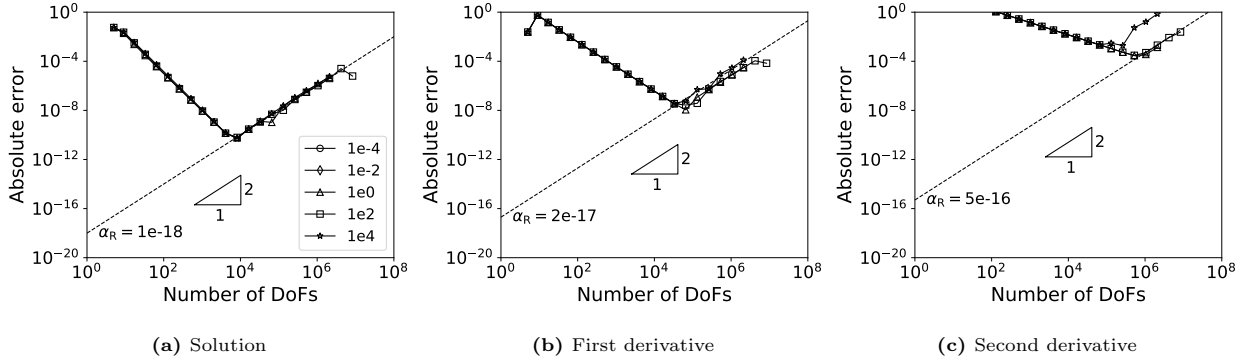


**Fig. 12.** Absolute errors for the benchmark diffusion equation but only imposed by Dirichlet boundary conditions using the standard FEM with scheme  $S$ ,  $c$  variant.

To clarify if the increase of  $\alpha_R$  for higher-order derivatives is caused by the magnitude of  $\|d\|_2$ , we divide the equation by  $\|d\|_2$ , which results in

$$-(d/\|d\|_2 u_x)_x = f/\|d\|_2. \quad (1)$$

For the above equation, the errors of the solution, first and second derivatives are shown in Fig. 13. It shows that  $\alpha_R$  also increases when  $c$  is relatively large.

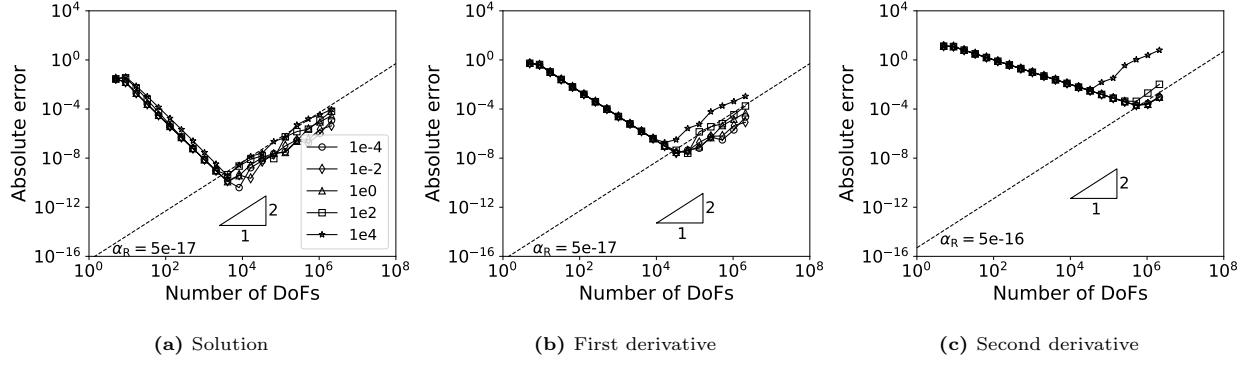


**Fig. 13.** Absolute errors for Eq. (1) using the standard FEM, no scaling,  $c$  variant.

*The mixed FEM.* Not using scaling, the errors are shown in Fig. 14. It shows that when  $c$  is relatively large,  $\alpha_R$  for the first and second derivatives increases. This is because the magnitude of the first derivative, which is  $\|du_x\|_2$ , increases with  $c$  when  $c > 1$ .

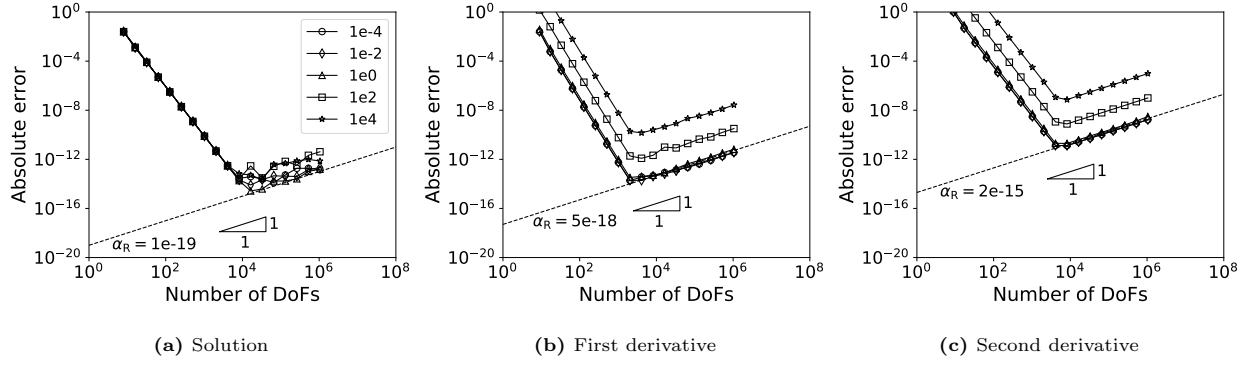


**Fig. 14.** Absolute errors for the benchmark diffusion equation using the mixed FEM with  $P_4/P_3^{\text{disc}}$  elements,  $v = -du_x$ , coefficient variant, no scaling.

If we use scheme  $M_1$  in [1], the errors are shown in Fig. 15, where the convergence behavior of  $\alpha_R$  is observed. Note that,  $\|v\|_2$  is  $\|du_x\|_2$  for the diffusion equation.

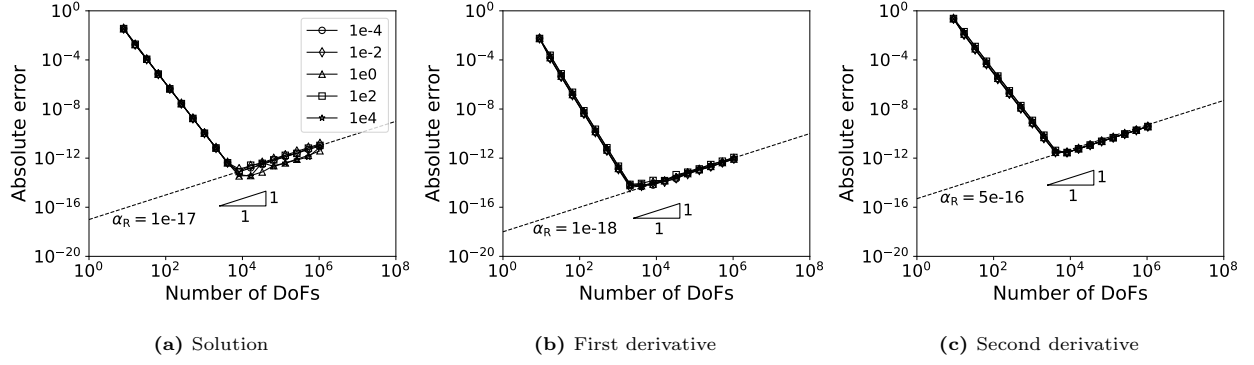


**Fig. 15.** Absolute errors for the benchmark diffusion equation using the mixed FEM with  $P_4/P_3^{\text{disc}}$  elements,  $v = -du_x$ , coefficient variant, scheme  $M_1$ .

### 1.5. The Helmholtz equation

For  $d(x) = 1 + 0.5 \sin(x)$ , we consider the influence of the magnitude of  $r(x)$  on the error. We consider  $r(x)$  as a constant, which ranges from 1 to  $10^8$ .

*The standard FEM.* We use  $P_2$  elements. The errors are shown in Fig. 16.

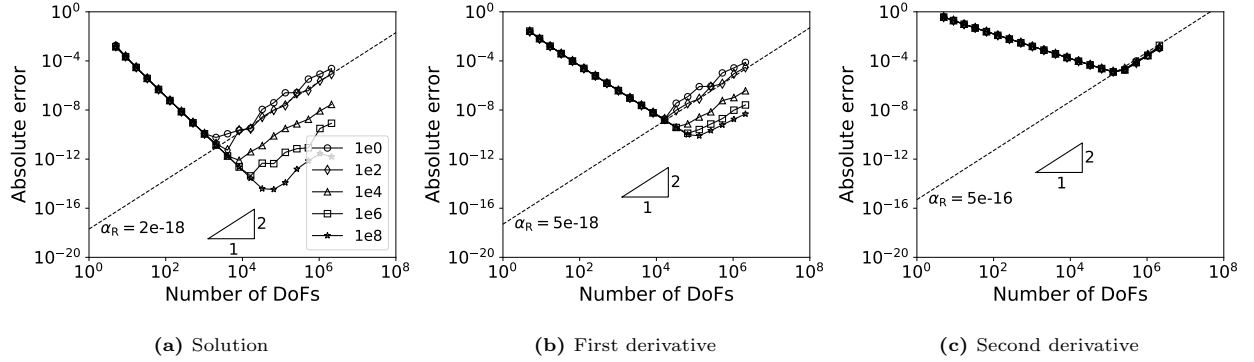


**Fig. 16.** Absolute errors for the Helmholtz equation using the standard FEM.

If we omit the diffusion part, i.e. concerning  $d(x) = 0$ , using the same set of  $r(x)$ , the errors are shown in Fig. 17.

Comparing Fig. 16 and Fig. 17, the slope 2 for the round-off error is led by the second-order derivative part in the differential equation.



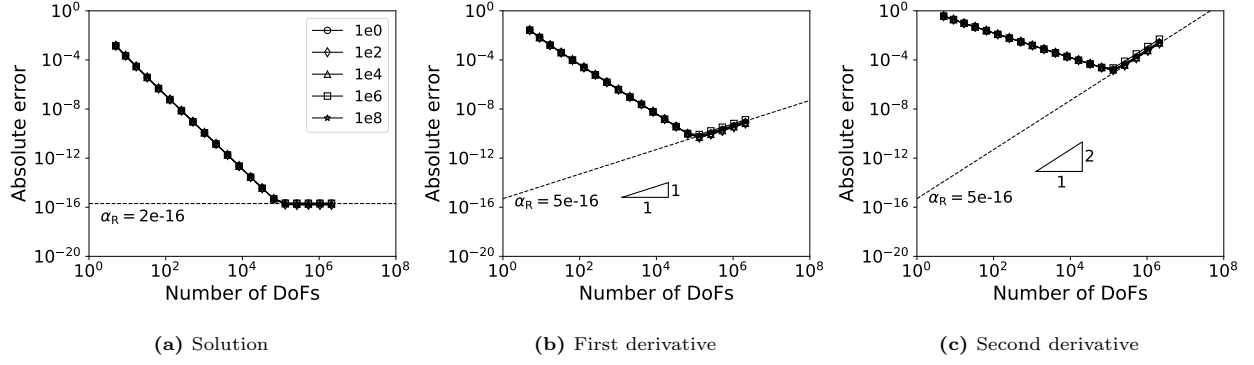


**Fig. 17.** Absolute errors for the Helmholtz equation, omitting the diffusion part, using the standard FEM.

### 1.6. The complex Helmholtz equation

For the benchmark Helmholtz equation, using both the standard FEM and the mixed FEM, the absolute errors for all *three* variables are shown in Fig. 18 and Fig. 19, respectively.

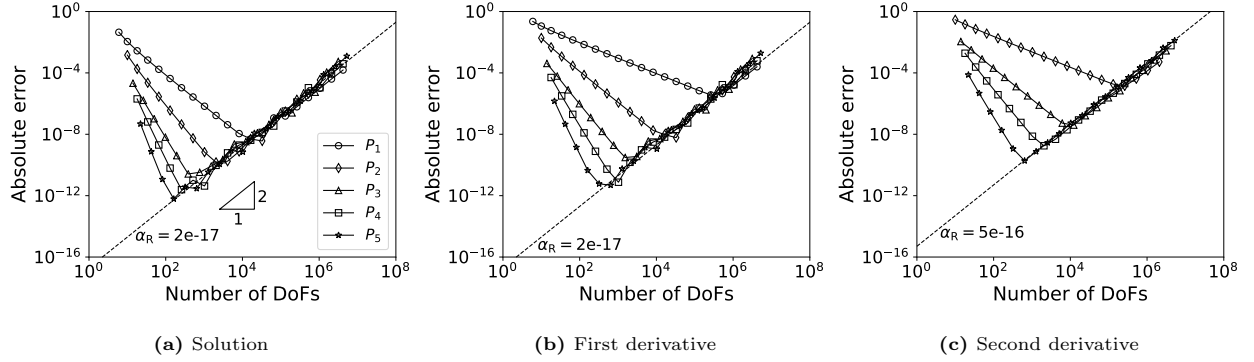


**Fig. 18.** Absolute errors for the benchmark Helmholtz equation using the standard FEM.

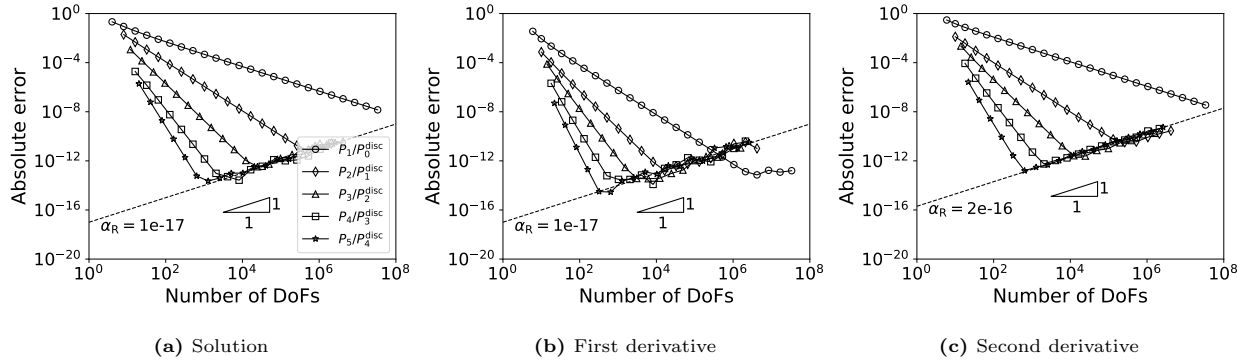


**Fig. 19.** Absolute errors for the benchmark Helmholtz equation using the mixed FEM.

## 2. $L_2$ norms and absolute errors for different cases

### 2.1. $L_2$ norms

The  $L_2$  norms of  $u$ ,  $u_x$  and/or  $u_{xx}(f)$  for different cases are shown in Fig. 20.

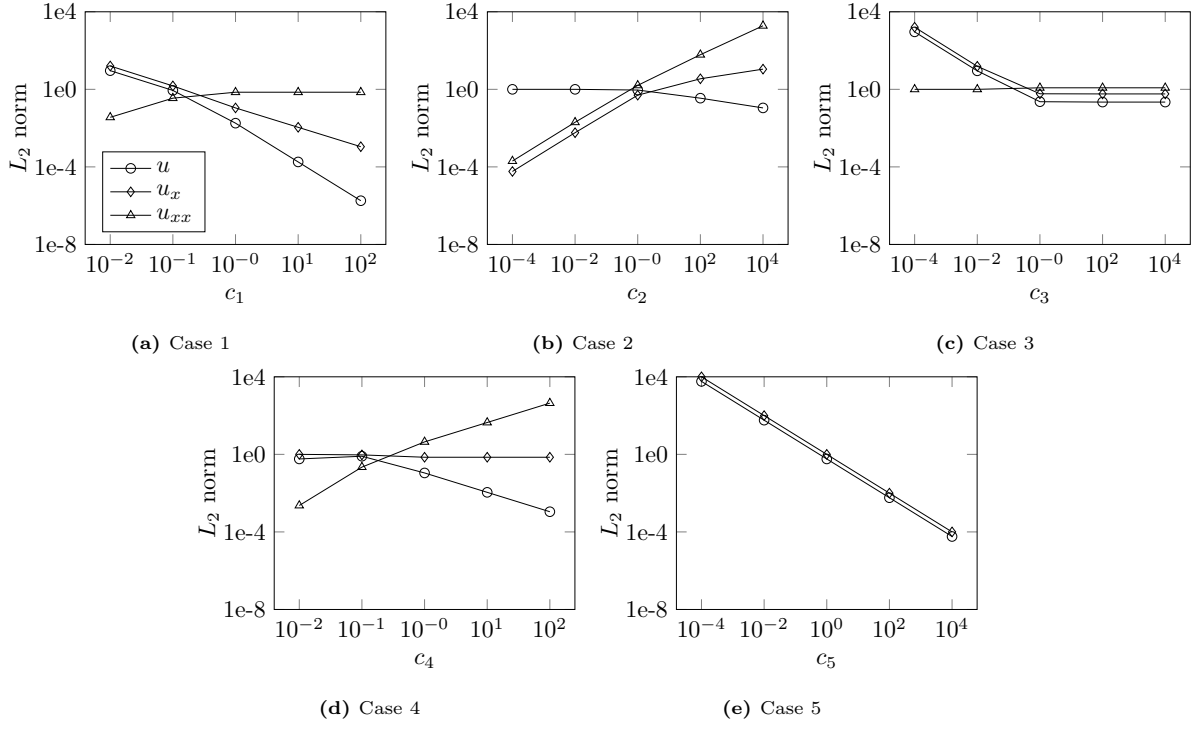


**Fig. 20.**  $L_2$  norms of  $u$ ,  $u_x$  and  $u_{xx}$  for different cases.

## 2.2. Absolute errors

### 2.2.1. The standard FEM

*Case 1.* For Case 1, using the standard FEM without scaling the right-hand side and scheme S, the absolute errors are shown in Figs. 21–22.

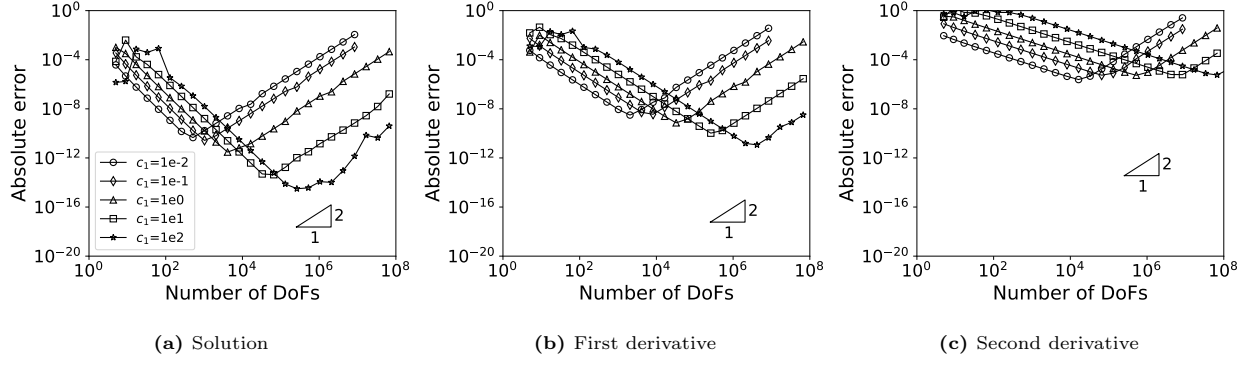


**Fig. 21.** Absolute errors for different  $c_1$  using the standard FEM without scaling the right-hand side.

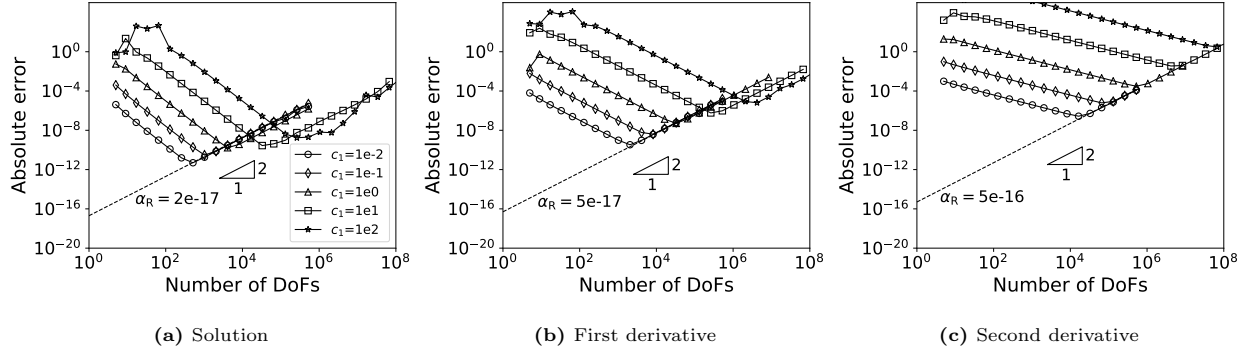


**Fig. 22.** Absolute errors for different  $c_1$  using the standard FEM with scheme S.

*Case 2.* For Case 2, using the standard FEM without scaling the right-hand side and scheme S, the absolute errors are shown in Figs. 23–24.

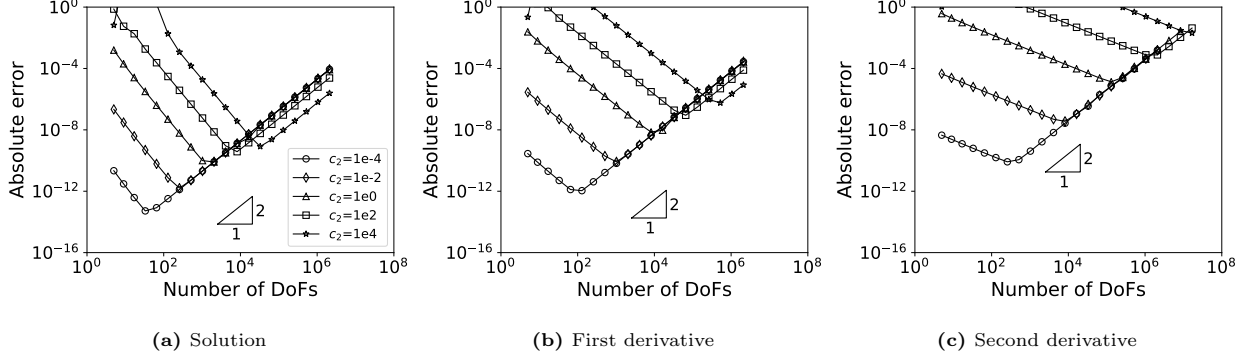


**Fig. 23.** Absolute errors for Case 2 using the standard FEM without scaling the right-hand side.

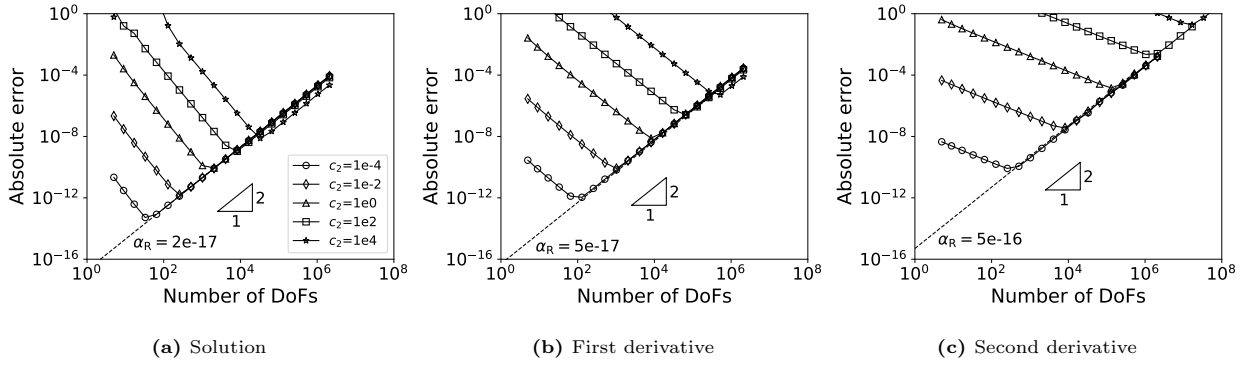


**Fig. 24.** Absolute errors for Case 2 using scheme S.

*Case 3.* For Case 3, using the standard FEM without scaling the right-hand side and scheme S, the absolute errors are shown in Figs. 25–26.

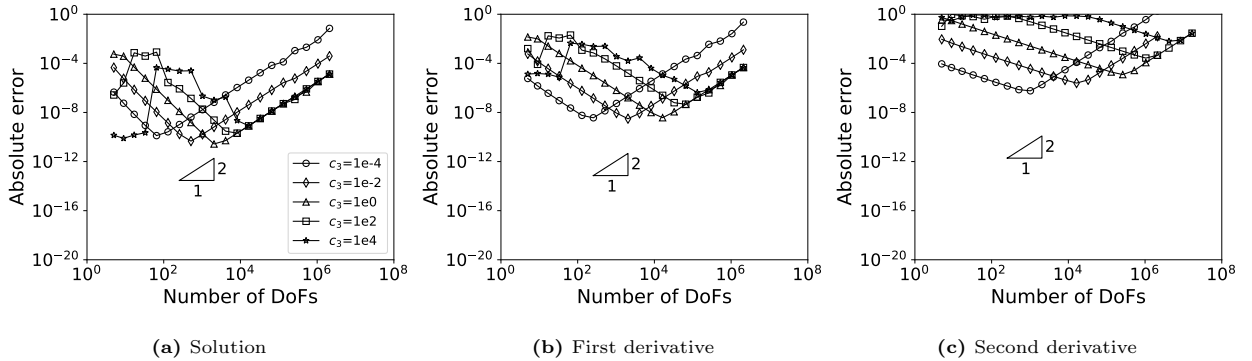


**Fig. 25.** Absolute errors for Case 3 using the standard FEM without scaling the right-hand side.

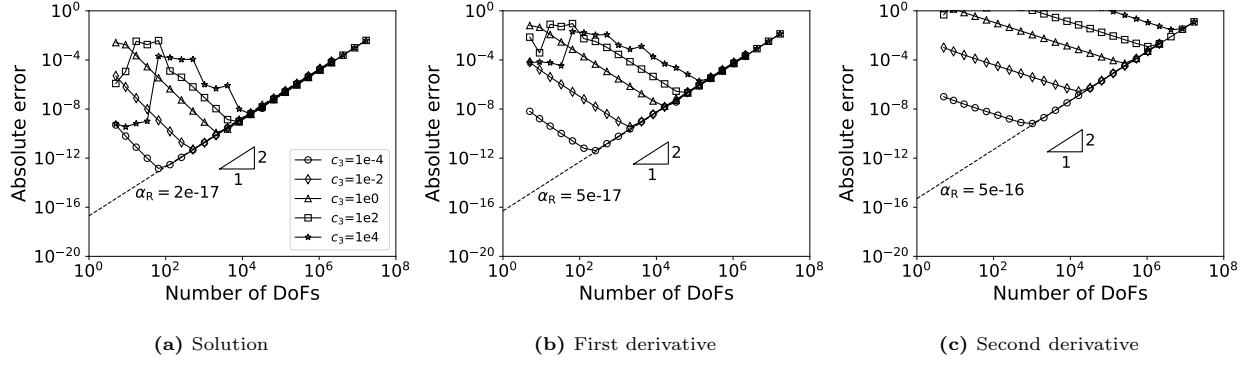


**Fig. 26.** Absolute errors of Case 3 using scheme  $S$ .

*Case 4.* For Case 4, using the standard FEM without scaling the right-hand side and scheme  $S$ , the absolute errors are shown in Figs. 27–28.

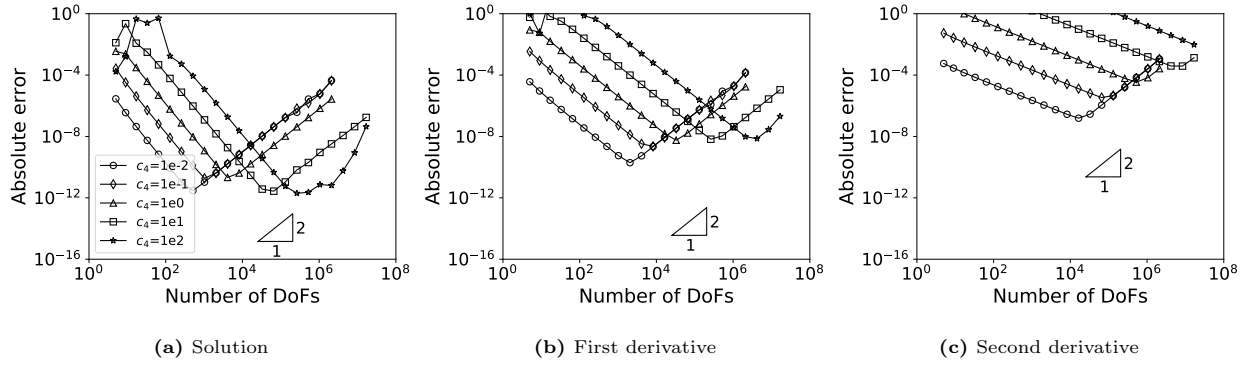


**Fig. 27.** Absolute errors for Case 4 using the standard FEM without scaling the right-hand side.

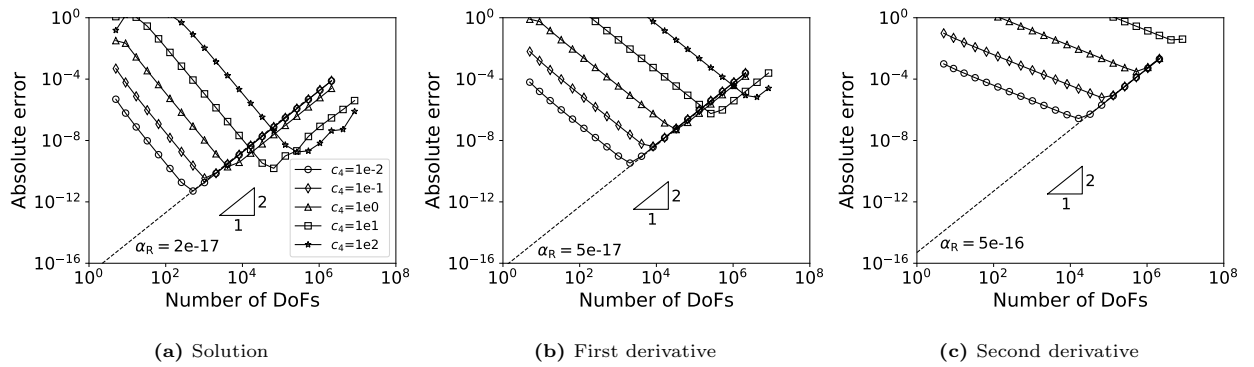


**Fig. 28.** Absolute errors of Case 4 using scheme  $S$ .

*Case 5.* For Case 5, using the standard FEM without scaling the right-hand side and scheme S, the absolute errors are shown in Figs. 29–30.

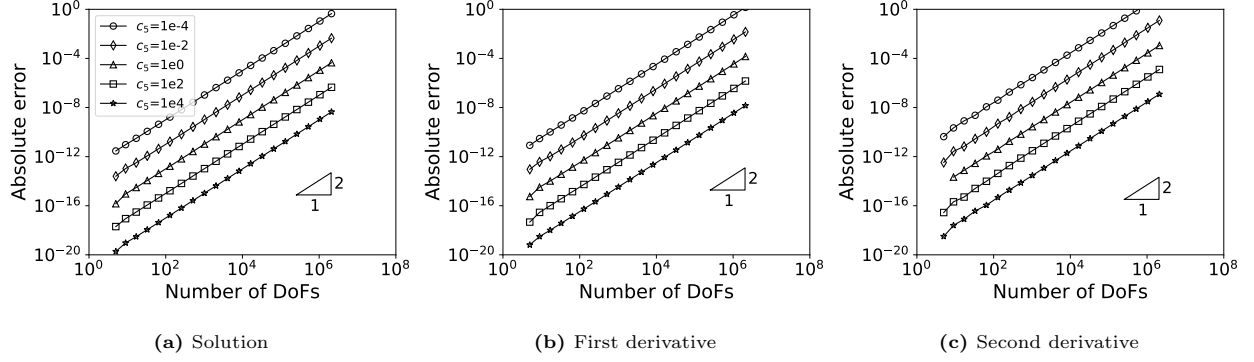


**Fig. 29.** Absolute errors for Case 5 using the standard FEM without scaling the right-hand side.

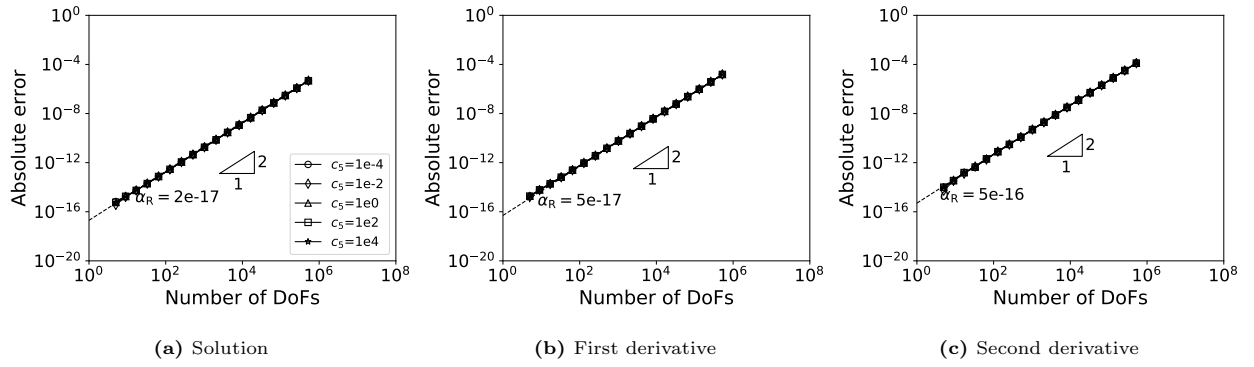


**Fig. 30.** Absolute errors of Case 5 using scheme S.

### 2.2.2. The mixed FEM

*Case 1.* For Case 1, using the mixed FEM without scaling the right-hand side and schemes  $M_1$  and  $M_2$ , the absolute errors are shown in Figs. 31–33.

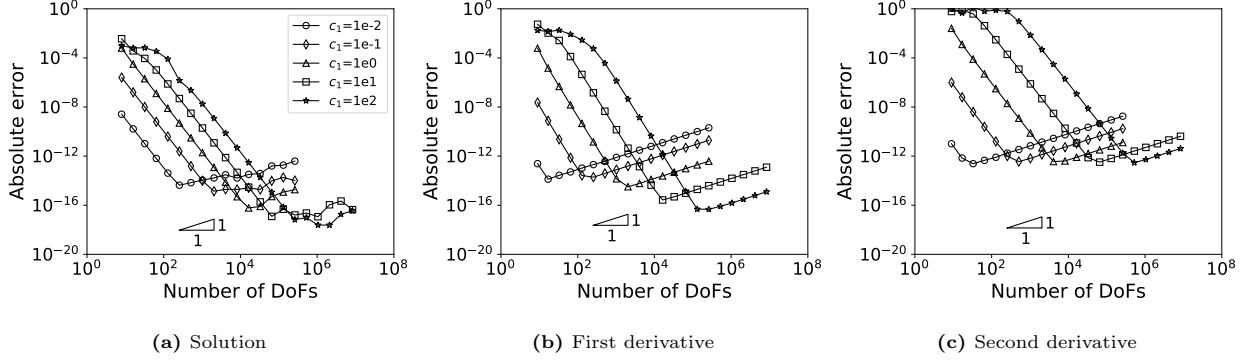


**Fig. 31.** Absolute errors for different  $c_1$  using the mixed FEM without scaling the right-hand side.

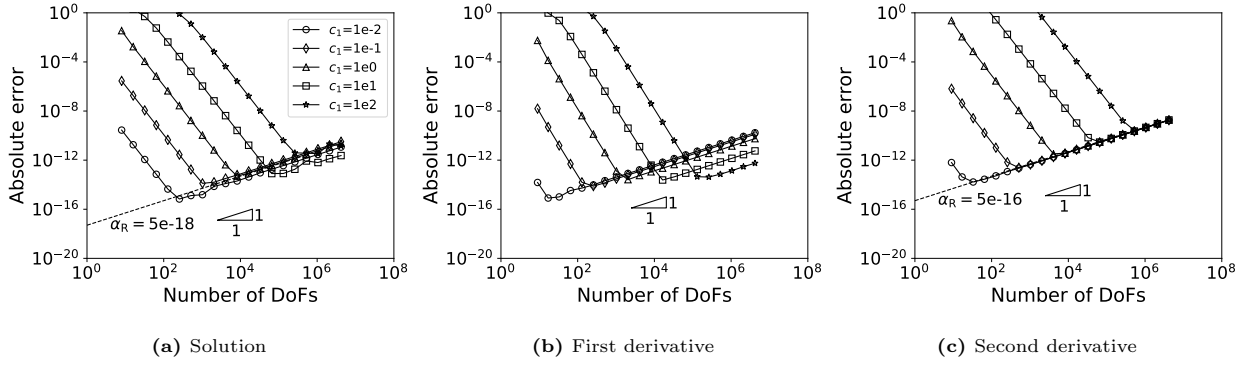


**Fig. 32.** Absolute errors for different  $c_1$  using the mixed FEM with scheme  $M_1$ .

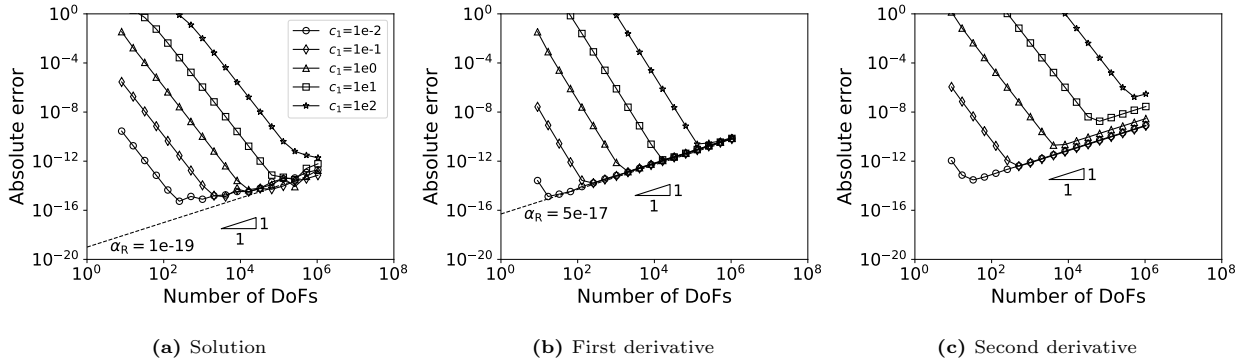


**Fig. 33.** Absolute errors for different  $c_1$  using the mixed FEM with scheme  $M_2$ .

*Case 2.* For Case 2, using the mixed FEM without scaling the right-hand side and schemes  $M_1$  and  $M_2$ , the absolute errors are shown in Figs. 34–36.

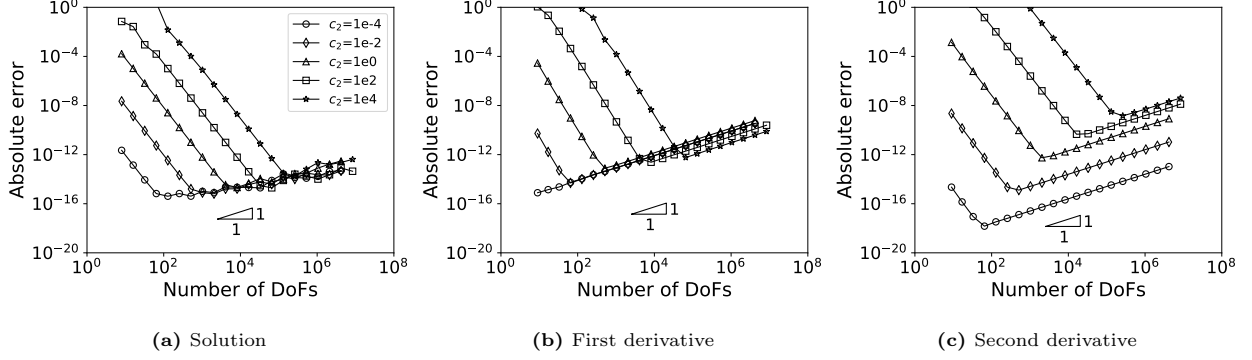


**Fig. 34.** Absolute errors for Case 2 using the mixed FEM without scaling the right-hand side.

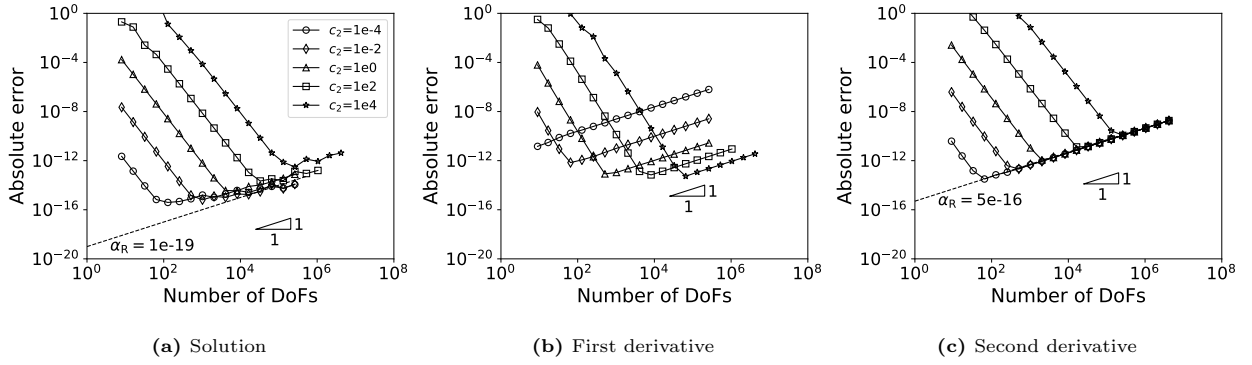


**Fig. 35.** Absolute errors for Case 2 using scheme  $M_1$ .

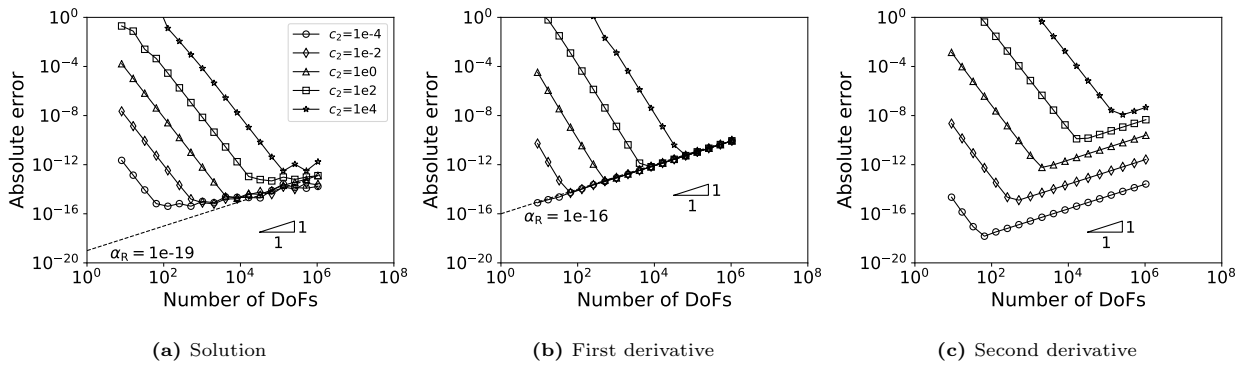


**Fig. 36.** Absolute errors for Case 2 using scheme  $M_2$ .



*Case 3.* For Case 3, using the mixed FEM without scaling the right-hand side and schemes  $M_1$  and  $M_2$ , the absolute errors are shown in Figs. 37–39.

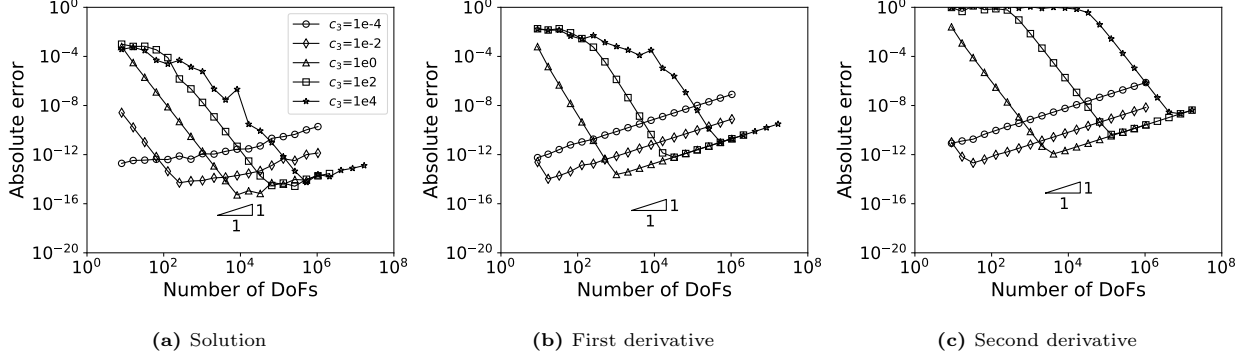


**Fig. 37.** Absolute errors for Case 3 using the mixed FEM without scaling the right-hand side.

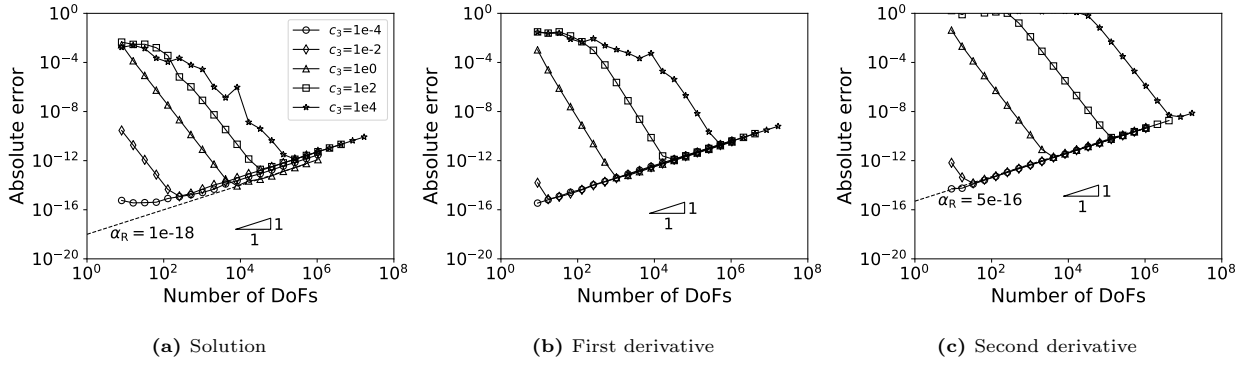


**Fig. 38.** Absolute errors for Case 3 using scheme  $M_1$ .

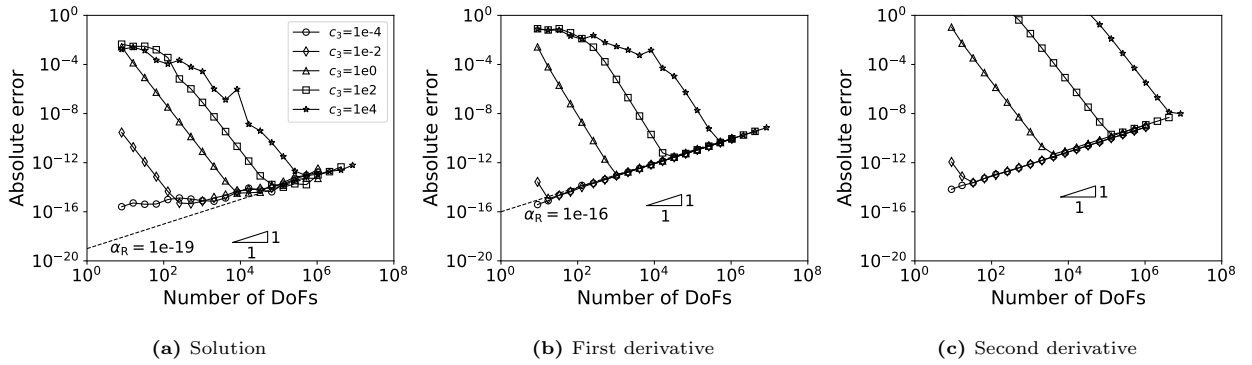


**Fig. 39.** Absolute errors for Case 3 using scheme  $M_2$ .

Case 4. For Case 4, using the mixed FEM without scaling the right-hand side and schemes  $M_1$  and  $M_2$ , the absolute errors are shown in Figs. 40–42.

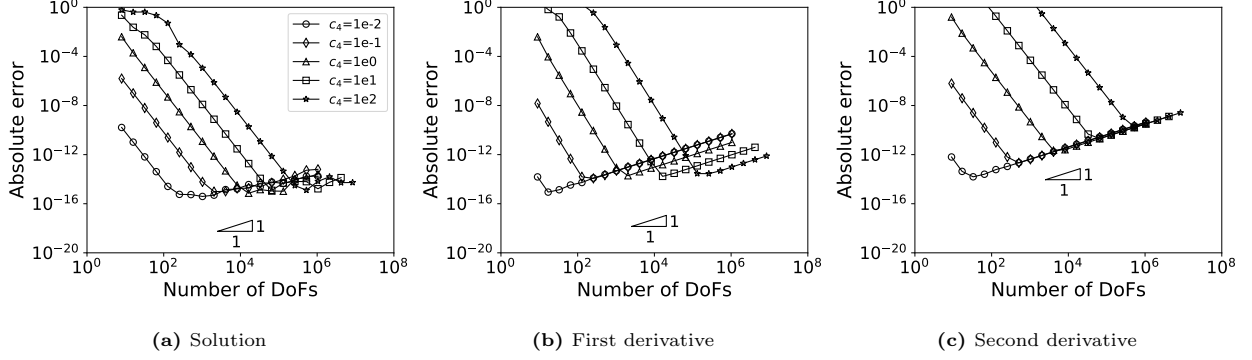


**Fig. 40.** Absolute errors for Case 4 using the mixed FEM without scaling the right-hand side.

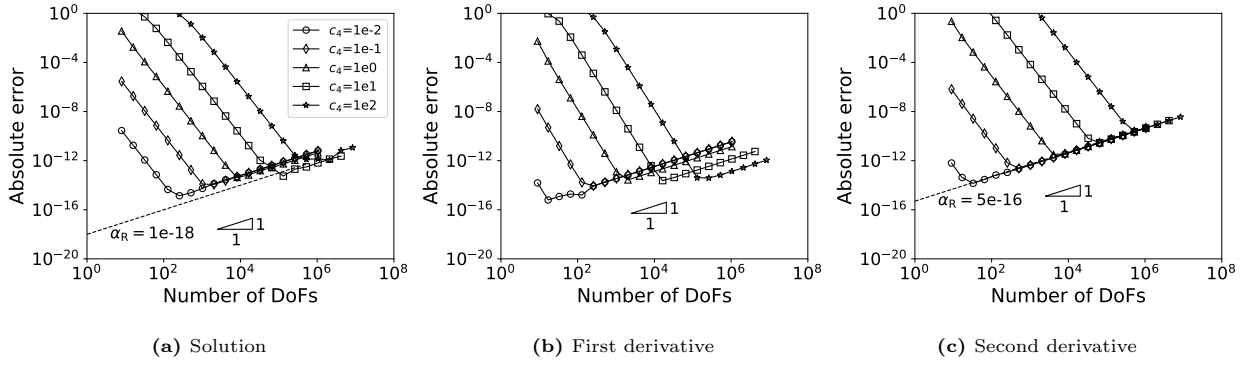


**Fig. 41.** Absolute errors for Case 4 using scheme  $M_1$ .

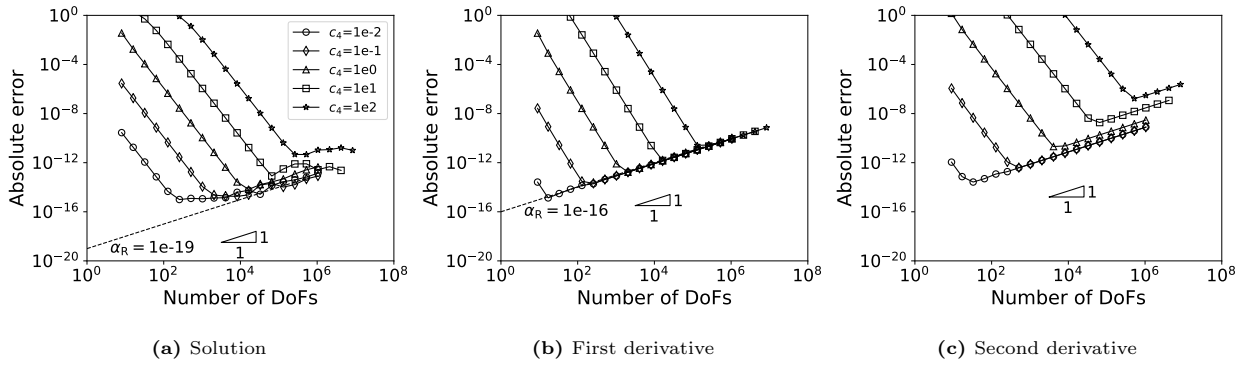


**Fig. 42.** Absolute errors for Case 4 using scheme  $M_2$ .

*Case 5.* For Case 5, using the mixed FEM without scaling the right-hand side and schemes  $M_1$ , the absolute errors are shown in Figs. 43–44.

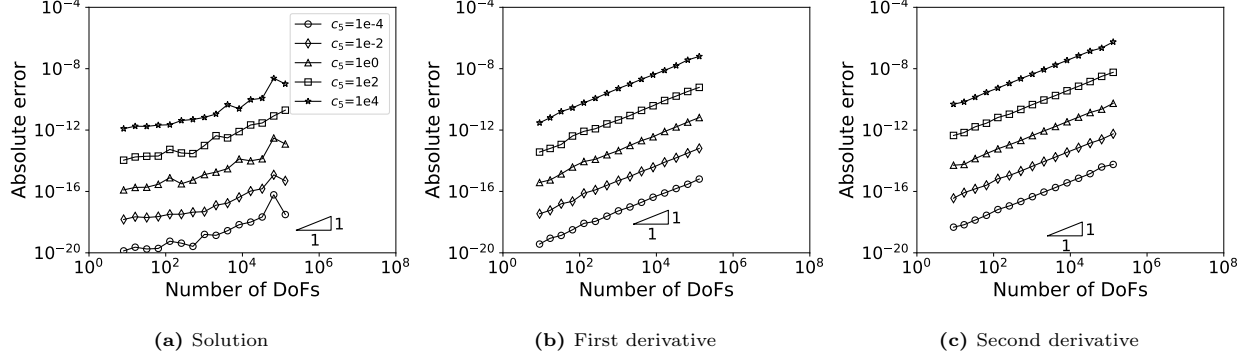


**Fig. 43.** Absolute errors for Case 5 using the mixed FEM without scaling the right-hand side.

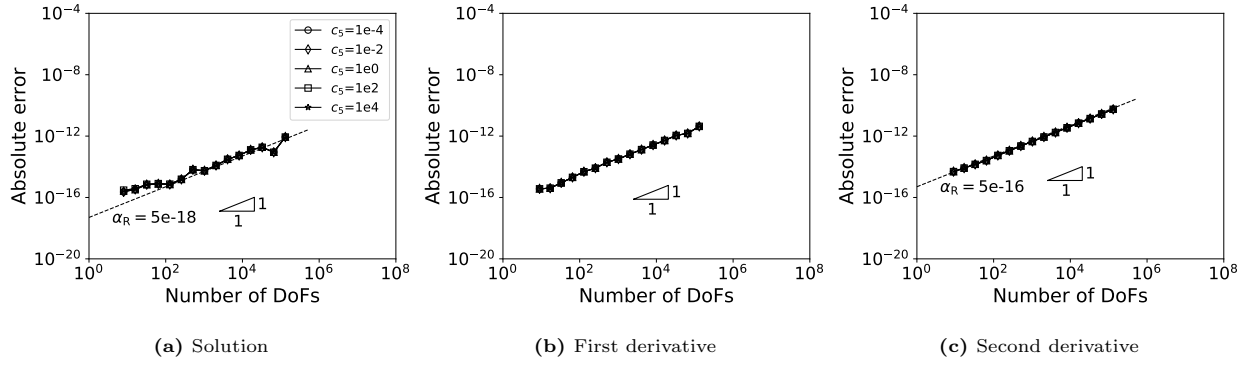


**Fig. 44.** Absolute errors for Case 5 using scheme  $M_1$ .

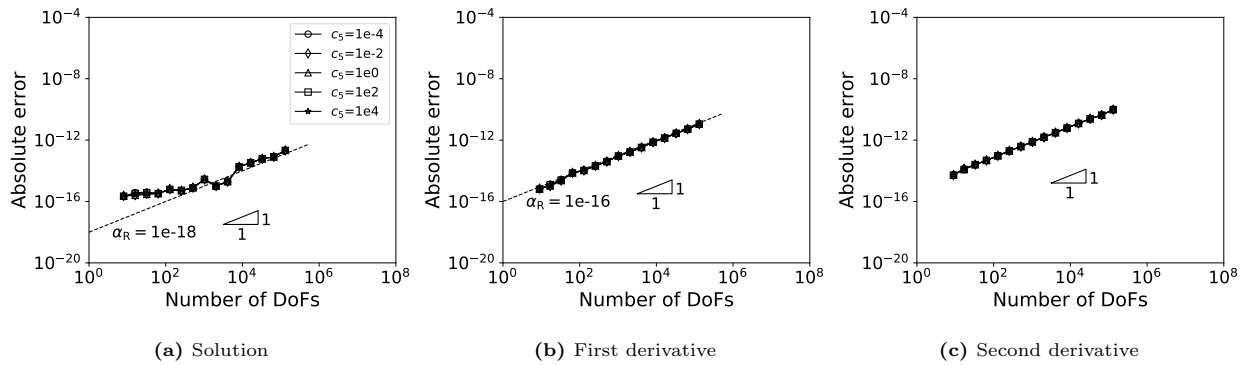


**Fig. 45.** Absolute errors for Case 5 using scheme  $M_2$ .

## References

- [1] Jie Liu, Matthias Möller, and Henk M Schuttelaars. Balancing truncation and round-off errors in practical fem: one-dimensional analysis. *arXiv preprint arXiv:1912.08004*, 2019.